Supporting Information

for

A facile avenue to conductive polymer brushes via cyclopentadiene-maleimide Diels–Alder ligation

Basit Yameen,[a] Cesar Rodriguez-Emmenegger,[a,b] Corinna M. Preuss,[a] Ognen Pop-Georgievski,[c] Elisseos Verveniotis,[d] Vanessa Trouillet,[e] Bohuslav Rezek [d] and Christopher Barner-Kowollik[a]*

[a] *Preparative Macromolecular Chemistry, Institut für Technische Chemie und Polymerchemie, Karlsruhe Institute of Technology (KIT), Engesserstr. 18, 76128 Karlsruhe, Germany and Institut für Biologische Grenzflächen, Karlsruhe Institute of Technology (KIT), Hermann-von-Helmholtz-Platz 1, 76344 Eggenstein-Leopoldshafen, Germany. Email: christopher.barner-kowollik@kit.edu, http://www.macroarc.de*

[b] *Zoological Institute, Department of Cell- and Neurobiology, Karlsruhe Institute of Technology (KIT), Haid-und-Neu-Str. 9, Karlsruhe, Germany.*

[c] *Institute of Macromolecular Chemistry, Academy of Sciences of the Czech Republic, Heyrovsky Square 2, 162 06 Prague 6, Czech Republic.*

[d] *Institute of Physics, Academy of Sciences of the Czech Republic, Cukrovarnicka 10, 16253, Prague, Czech Republic.*

[e] *Institute for Applied Materials (IAM) and Karlsruhe Nano Micro Facility (KNMF), Karlsruhe Institute of Technology (KIT), Hermann-von-Helmholtz-Platz 1, 76344 Eggenstein-Leopoldshafen, Germany.*

Experimental Details

Materials and methods

Cyclopentadienyl (Cp) end capped P3HT (P3HT-Cp, **4**) was synthesized according to a previously reported procedure.[1] Dopamine/HCl (98.5%) and APTES (99%) were used as received from Sigma-Aldrich. THF (99.5%) was used as received from VWR. Dry THF was obtained from Acros Organics. Triethylamine (TEA) was refluxed overnight with CaH_2, distilled and stored under N_2(g). 4-Maleimidobutyroyl chloride (**2**) was synthesized from 4-maleimidobutyric acid according to a previously reported procedure.[2] PET foil (0.1 mm) was from Goodfellow (England).

X-Ray photoelectron spectroscopy

XPS (X-ray photoelectron spectroscopy) measurements were performed using a K-Alpha XPS spectrometer (ThermoFisher Scientific, East Grinstead, UK). All the samples were analyzed using a microfocused, monochromated Al K_α X-ray source (400 μm spot size). The kinetic energy of the electrons was measured by a 180° hemispherical energy analyzer operated in constant analyzer energy mode (CAE) at 50 eV pass energy for elemental spectra. Data acquisition and processing using the Thermo Avantage software are described elsewhere.[3] The spectra were fitted with one or more Voigt profiles (binding energy uncertainty: ± 0.2 eV). The analyzer transmission function, Scofield sensitivity factors,[4] and effective attenuation lengths (EALs) for photoelectrons were applied for quantification. EALs were calculated using the standard TPP-2M formalism.[5] All spectra were referenced to the C1s peak of hydrocarbon at 285.0 eV binding energy controlled by means of the well-known photoelectron peaks of metallic Cu, Ag, and Au.

Spectroscopic ellipsometry

Ellipsometry measurements were performed on a Spectroscopic Imaging Auto-Nulling Ellipsometer EP³-SE (Nanofilm Technologies GmbH, Germany) in the wavelength range of λ = 398.9 – 900.0 nm (source Xe-arc lamp, wavelength step ~10 nm) prior to and after every deposition/modification step. To increase the measurement precision, a 5× objective and position calibrated sample stage were utilized to perform repeated measurements from the same area of

1×2 mm^2 on the sample. All measurements were performed at an angle of incidence AOI = 70 °, except the measurements intended for acquiring optical constants of the P3HT and APTES polymer layers which were performed at AOI = 65 °, 70 ° and 75 °.

The ellipsometric data were fitted with multilayer models using the EP^4-SE analysis software (Accurion GmbH, Germany). The thickness and refractive indexes n of APTES and maleimide layers were obtained from simultaneous fitting using Cauchy dispersion function $n = A_n + B_n/\lambda^2$ (APTES: $A_n = 1.413$, $B_n = 6265$ nm^2) The parameters for maleimide (MI) ($A_n = 1.521$, $B_n = 1100$ nm^2) were calculated by the method proposed by Askadskii.[6] The optical dispersion function of PDA was taken from elsewhere. [7] The optical dispersion function of P3HT layer, which absorbs in UV-VIS region, was determined by multiple sample analyses combined with the interference enhancement method.[7,8] For this purpose, P3HT films with thickness ranging from 10 to 135 nm were spin coated on 250 nm thick SiO_2/Si substrates. The presence of a thick transparent SiO_2 layer between the silicon substrate and P3HT film causes damped interference oscillations in the measured ellipsometric spectra (Ψ and Δ), enhancing the sensitivity to both film thickness and the film optical constants.[7] The acquired ellipsometric data from the four P3HT films of different thickness were simultaneously analyzed using a superposition of Cauchy dispersion function and three Lorentz oscillators characterized by center energy (E_n), amplitude (Am_n) and broadening (Br_n) for the optical dispersion function of P3HT. Via such a procedure, unique solutions for the fitted parameters can be obtained due to significant decorrelation of the film thickness and optical constants. The accordingly obtained Cauchy and Lorentz oscillator parameters of the P3HT films are: $A_n = 1.623 \pm 0.009$, $B_n = 7790 \pm 1600$, $E_1 = 2.250 \pm 0.012$ [eV], $Br_1 = 0.311 \pm 0.029$ [eV], $Am_1 = 0.687 \pm 0.175$ [(eV)²], $E_2 = 2.495 \pm 0.011$ [eV], $Br_2 = 0.407 \pm 0.052$ [eV], $Am_2 = 1.466 \pm 0.302$ [(eV)²], $E_3 = 2.888 \pm 0.023$ [eV], $Br_3 = 0.516 \pm 0.063$ [eV] and $Am_3 = 0.586 \pm 0.145$ [(eV)²] (where E_n, Br_n, and Am_n are the center energy, broadening and amplitude, respectively, of the oscillators). The Si/SiO_2 substrates were modeled using the dispersion functions published by Herzinger *et al.*[9] The gold layer was modeled as bulk gold with a software predefined optical function since at thickness of 200 nm and higher the layer is practically non-transparent at the employed wavelength.

Resulting parameters are listed in Table S1. The corresponding P3HT film optical constants (refractive index and extinction coefficient) are shown in Fig. S3. Fig. S4 to S7 show the

measured and fitted Δ and Ψ spectra. The accordingly determined optical dispersion function was used for the thickness determination of the P3HT films formed via ligation chemistry to maleimide-carrying substrates.

Surface profilometry

P3HT thickness control measurements were performed on a Tencor P-10 Surface Profiler (Texas, USA). Step height profiles were taken over a groove on the P3HT films. The step height profiles of 1 mm long scans were recorded at speed of 20 μm/s and sampling rate of 200 Hz at maximum stylus force of 0.02 N.

Scanning probe microscopy

All scanning probe microscopy experiments were performed with a N-TEGRA system by NT-MDT. Conductive Cr/Pt coated silicon probes (Multi 75G by BudgetSensors) were used in all the studies. Kelvin-Probe Force microscopy in the 2-pass regime[10] was used to detect electric potential shifts on the samples after each chemical modification performed on them. Lift height during the 2nd pass and scan rate were 10 nm and 1 Hz, respectively. Relative humidity and temperature during all AFM/KFM experiments were in the ranges of 29-31% and 23–25 °C. Each data point as depicted in the Fig. 2 in the main manuscript was calculated from a 5x5 μm^2 KFM potential map.

Substrate preparation

One side polished silicon (Si) wafers (CZ, orientation <100>, B-doped, resistivity 1-100 Ω cm) with ~1.5 nm natural oxide and ~250 nm (SHE-Europe Ltd., Scotland) thermal silicon dioxide (SiO_2) over-layer were cut into 1.2 × 2.4 cm^2 pieces, sonicated in methanol and deionized water (Milli Q system, Millipore) for 15 min, immersed in a mixture of 25% ammonia, 30% hydrogen peroxide and water (1:1:5 v/v/v) heated at 70 °C for 10 min and finally thoroughly rinsed with water. Dry samples were exposed to air plasma (25W) for 5 min just before polymer deposition. Gold coated substrates consisted of a Si support, ~2 nm of titanium adhesion layer and ~200 nm of gold layer. These were cleaned by sonication in methanol and water for 15 min, blow dried and exposed to air-plasma before use.

APTES functionalized Si substrates (1)

APTES was functionalized at the surface of plasma activated Si substrates. A glass Petri dish containing activated Si substrates (1×1 cm^2) was placed in a desiccator along with APTES in a separate glass vial. The entire system was kept under vacuum for 2 h. The Si substrates were subsequently annealed at 130 °C for 4 h before rinsing them with toluene, dichloromethane, acetone and methanol. The resulting APTES functionalized Si substrates were dried with a stream of N_2(g) and stored in a dessicator under inert atmosphere.

Polydopamine (PDA) coated Si (7), Au (11) and PET (14) substrates

PDA was deposited from a 2 $mg \cdot mL^{-1}$ solution of dopamine hydrochloride in an air-saturated 10 mM Tris-HCl (pH 8.5) buffer.[11] The deposition of PDA on different substrates was performed in open glass dishes under controlled stirring that provided a continuous supply of oxygen through the air/solution interface. The flat substrates were kept vertical to suppress microparticle sedimentation.[12] The coated surfaces were finally rinsed with water, sonicated in water for 15 min and dried in a stream of nitrogen.

Maleimide functionalized substrates (3, 8, 12, 15)

The APTES functionalized Si substrate (**1**) and PDA coated Si (**7**), Au (**11**), and PET (**14**) substrates were separately immersed in 55mM THF solution of TEA. Equal volume of a 50 mM solution of 4-maleimidobutyroyl chloride (**2**) in dry THF was subsequently added under inert atmosphere. The reaction was allowed to proceed for 4 h. The substrates were subsequently rinsed with THF to remove any physisorbed **2** and methanol to remove the quaternary ammonium salt, which formed during the reaction. The substrates were dried by employing a stream of N_2(g) and stored at 4 °C under inert atmosphere.

P3HT brush functionalized substrates via Cp-maleimide Diels–Alder click ligation (5, 9, 13, 16)

The maleimide functionalized substrates **(3, 8, 12, 15)** were immersed in a THF solution of P3HT-Cp (5 $mg \cdot mL^{-1}$) and allowed to react overnight under ambient conditions. The substrates were subsequently rinsed with THF, dried by employing a stream of N_2(g), and stored in the dark.

XPS spectra for the PDA assisted P3HT brushes functionalized substrates

The maleimide functionalization of the all surfaces is evidenced by the appearance of a signal assigned to the N-C=O bond at 288.8 eV.[13] After the Cp-maleimide ligation, the decrease of the N-C=O bond signal with an associated increase in the intensity of the of C-C and C-H bonds signals reflects the incorporation of the P3HT polymer at the surface. The grafting of P3HT-Cp (**4**) to the surfaces *via* Cp-maleimide Diels–Alder ligation is further verified as the appearance of the signal corresponding to the sulfur.[14] Furthermore, the negative control experiments displayed no change in the C 1s and sulfur signal, which excludes any contribution from physisorption of the P3HT chains at the surface.

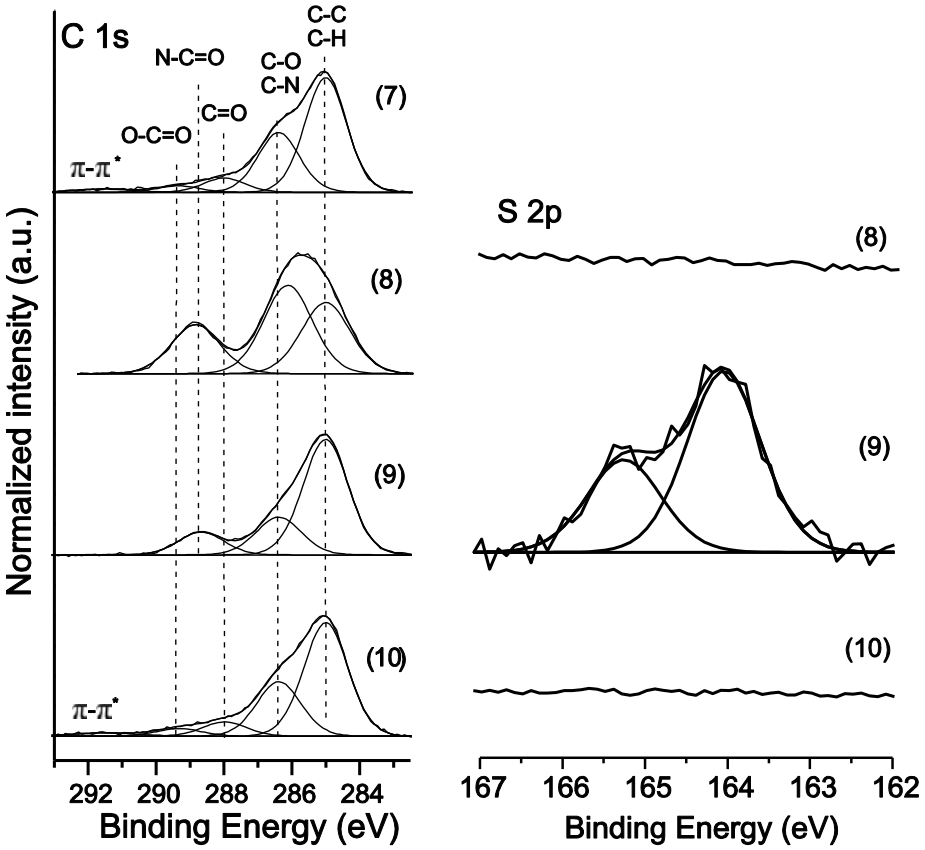

Fig. S1 Monitoring of P3HT brush fabrication on an Si substrate (via PDA chemistry, Scheme 1B) by C 1s (left) and S 2p (right) high resolution XPS analysis.

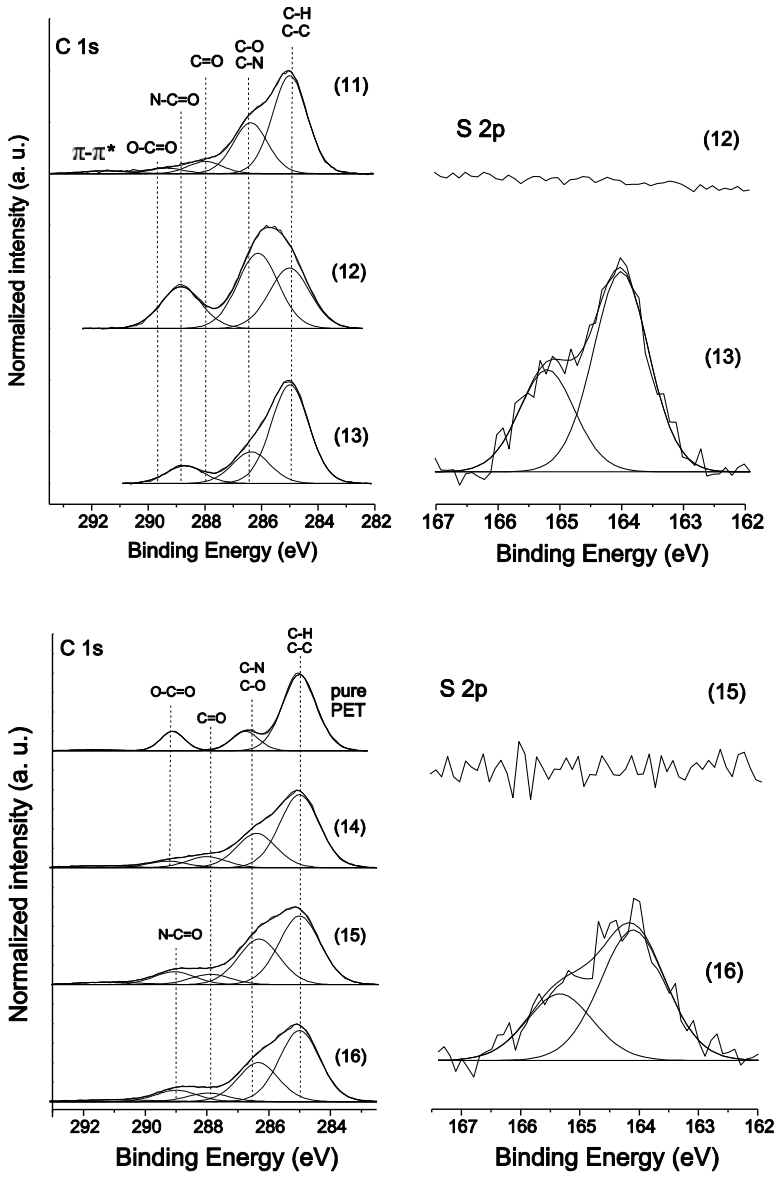

Fig. S2 XPS monitoring of P3HT brush fabrication on an Au substrate (top left C 1s and top right S 2p) and on PET substrate (bottom left C 1s and bottom right S 2p) via PDA coating as depicted in the Scheme 1B.

The C 1s spectrum for pure PDA (**7**) shows characteristic peaks that were consistent with previous findings.[12] The XPS data for the PDA-assisted PET functionalization also confirmed the successful surface functionalization. For reference, the C 1s spectrum for pure PET is also depicted (Fig. S2). The characteristic PET spectrum was consistent with previous findings.[15]

For the Si substrates (**1**, **3**, **5**), the S 2s orbital signal was chosen as the representative signal for sulfur as the S 2p orbital signal is covered by the plasmon loss structure of the Si signal, which appears in the same region. The masking of the Si surface by the PDA layer (19 nm) made it possible to observe the more characteristic S 2p orbital signals for the rest of the samples.

Fabrication of spin-coated P3HT films for SE analysis

P3HT films were spin-coated from 20, 10, 5, and 2.5 mg·mL^{-1} P3HT (M_n 6.2 kDa, $Đ$ 1.1) solutions in chloroform (2000 rpm·min^{-1}) to obtain *ca.* 135, 45, 20 and 10 nm thick layers, respectively. The coated substrates were dried under vacuum at ambient temperature for 1 h.

P3HT dispersion function by spectroscopic ellipsometry

Table S1. Ellipsometry thicknesses and parameters of the optical dispersion function of P3HT films obtained from the combinatorial interference enhancement and multiple sample analysis.

Sample S1 thickness:	11.8 ± 0.2 nm
Sample S2 thickness:	22.1 ± 0.2 nm
Sample S3 thickness:	52.0 ± 0.3 nm
Sample S4 thickness:	137 ± 1 nm
MSE	6.8
Cauchy parameters:	
A_n	1.623 ± 0.009
B_n	7790 ± 1600 [nm^2]
Lorentz oscillators:	
E_1	2.250 ± 0.012 [eV]
Br_1	0.311± 0.029 [eV]
Am_1	0.687 ± 0.175 [(eV)^2]
E_2	2.495 ± 0.011 [eV]
Br_2	0.407± 0.052 [eV]
Am_2	1.466 ± 0.302 [(eV)^2]
E_3	2.888 ± 0.023 [eV]
Br_3	0.516 ± 0.063 [eV]
Am_3	0.585 ± 0.145 [(eV)^2]

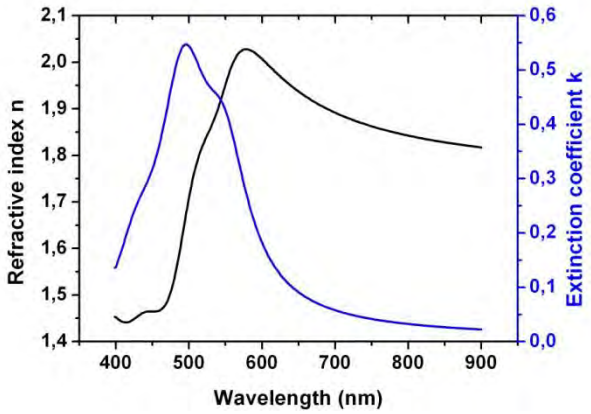

Fig. S3 Optical constants obtained for the P3HT films using the parameters reported in Table S1. The black curve corresponds to the refractive index (*n*), and blue curve corresponds to the extinction coefficient (*k*) of P3HT.

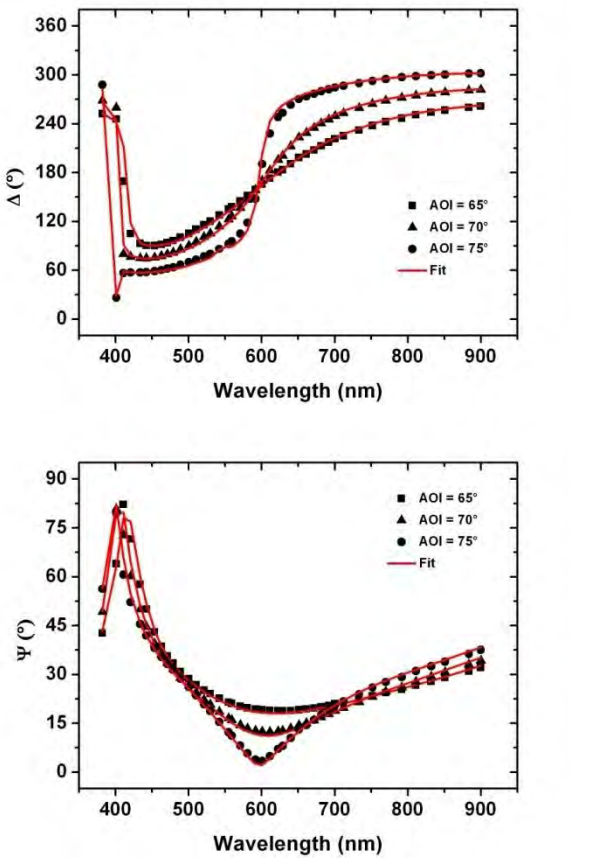

Fig. S4 Experimental (■ at AOI=65°), (▲ at AOI=70°), (● at AOI=75°) and fitted (─) Δ and Ψ spectra obtained by multiple sample analysis for P3HT layer S1 (11.8 ± 0.2 nm).

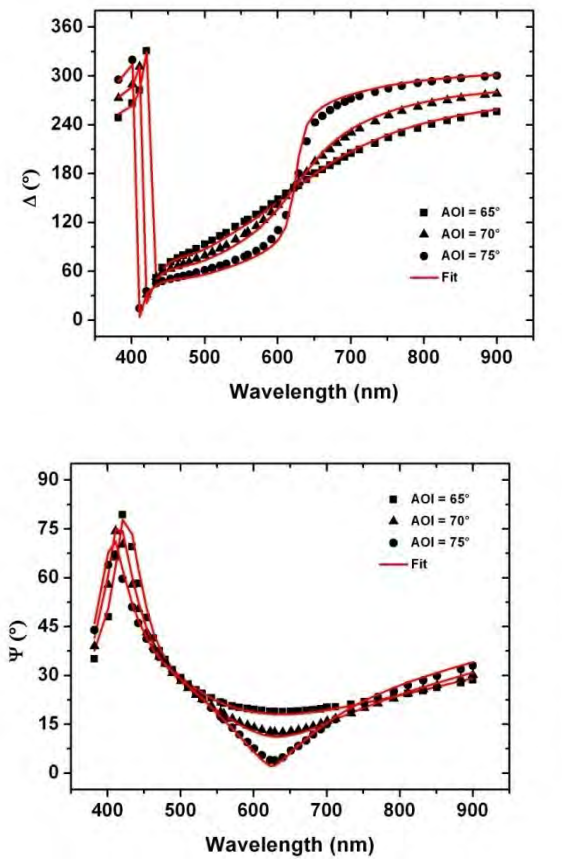

Fig. S5 Experimental (■ at AOI=65°), (▲ at AOI=70°), (● at AOI=75°) and fitted (─)(─) Δ and Ψ spectra obtained by multiple sample analysis for P3HT layer S2 (22.1 ± 0.2 nm).

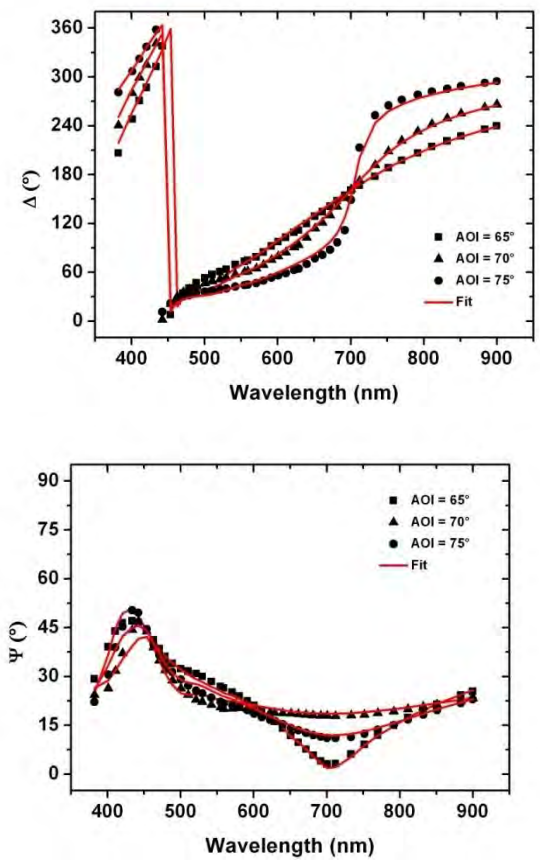

Fig. S6 Experimental (■ at AOI=65°), (▲ at AOI=70°), (● at AOI=75°) and fitted (─)(─) Δ and Ψ spectra obtained by multiple sample analysis for P3HT layer S3 (52.0 ± 0.3 nm).

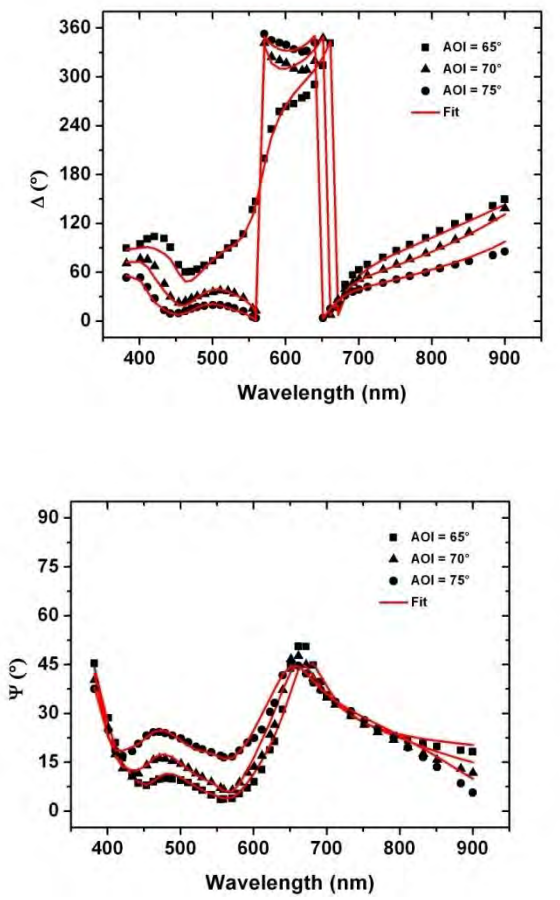

Fig. S7 Experimental (■ at AOI=65°), (▲ at AOI=70°), (● at AOI=75°) and fitted (—)(—) Δ and Ψ spectra obtained by multiple sample analysis for P3HT layer S4 (137.0 ± 1 nm).

Comparison between ellipsometry and stylus profilometry measurements of P3HT layer thickness

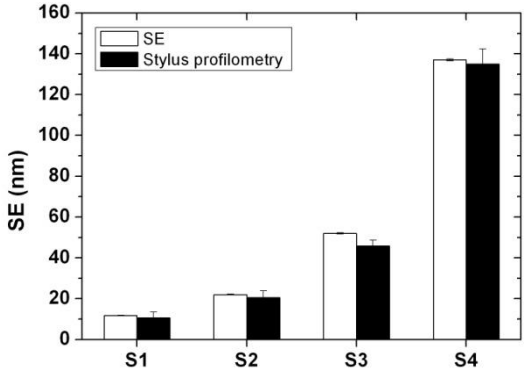

Fig. S8 Comparison of P3HT film thickness obtained from spectroscopic (white bars) and ellipsometry stylus profilometry (black bars).

Table S2: Ellipsometric thinknesses of the fabricated P3HT brushes fabricated via Cp-maleimide Diels–Alder ligation.

Sample (ID) Via silane chemistry	Thickness of the layer (nm)	Sample (ID) Via PDA coating	Thickness of the layer (nm)
1	3.5	**11**	19
3	2.2	**12**	1.7
5	4.3	**13**	4.7

Scanning probe microscopy

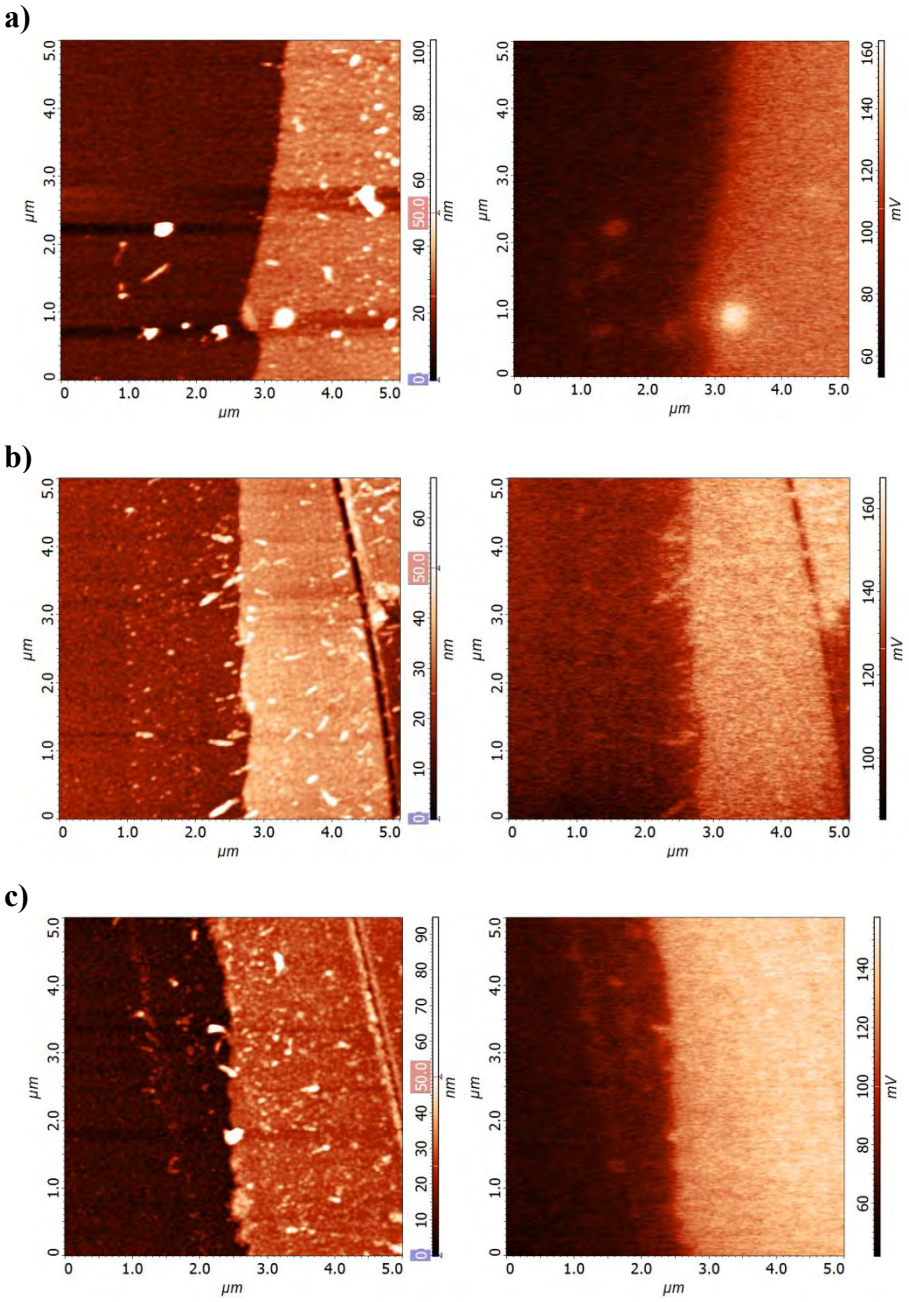

Fig. S9 The AFM topographies (left) and KFM potential maps (right) for PDA coated gold substrate **11** (a), maleimide functionalized substrate **12** (b) and P3HT brush-functionalized substrate **13** (c).

References

1) B. Yameen, N. Zydziak, S. M. Weidner, M. Bruns and C. Barner-Kowollik, *Macromolecules*, 2013, **46**, 2606.
2) A. Herrmann, G. Mihov, G. W. M. Vandermeulen, H.-A. Klok and K. Müllen, *Tetrahedron*, 2003, **59**, 3925.
3) K. L. Parry, A. G. Shard, R. D. Short, R. G. White, J. D. Whittle and A. Wright, *Surf. Interface Anal.,* 2006, **38**, 1497.
4) S. Tanuma, C. J. Powell and D. R. Penn, *Surface and Interface Analysis*, 1994, **21**, 165.
5) J. H. Scofield, *Journal of Electron Spectroscopy and Related Phenomena*, 1976, **8**, 129.
6) A. A. Askadskii, *Physical Properties of Polymers: Prediction and Control*., Gordon and Breach Publ.: Amsterdam, 1996; Vol. 2.
7) O. Pop-Georgievski, S. Popelka, M. Houska, D. Chvostova, V. Proks and F. Rypacek, *Biomacromolecules*, 2011, **12**, 3232.
8) W. A. McGahan, B. Johs and J. A. Woollam, *Thin Solid Films*, 1993, **234**, 443; J. N. Hilfiker, N. Singh, T. Tiwald, D. Convey, S. M. Smith, J. H. Baker and H. G. Tompkins, *Thin Solid Films*, 2008, **516**, 7979.
9) C. M. Herzinger, B. Johs, W. A. McGahan, J. A. Woollam and W. Paulson, *J. Appl. Phys.*, 1998, **83**, 3323.
10) M. Nonnenmacher, M. P. O'Boyle and H. K. Wickramasinghe, *Appl. Phys. Lett.*, 1991, **58**, 2921; E. Verveniotis, A. Kromka, M. Ledinský and B. Rezek, *Diamond Relat. Mater.*, 2011, **24**, 39; E. Verveniotis, A. Kromka and B. Rezek, *Langmuir*, 2013, doi:10.1021/la4008312.
11) H. Lee, S. M. Dellatore, W. M. Miller, P. B. Messersmith, *Science*, 2007, **318**, 426.
12) O. Pop-Georgievski, N. Neykova, V. Proks, J. Houdkova, E. Ukraintsev, J. Zemek, A. Kromka, F. Rypaček, *Thin Solid Films*, 2013, http://dx.doi.org/10.1016/j.tsf.2012.11.128; O. Pop-Georgievski, D. Verreault, M.-O. Diesner, V. Proks, S. Heissler, F. Rypáček, P. Koelsch, *Langmuir*, 2012, **28**, 14273. O. Pop-Georgievski, S. Popelka, M. Houska, D. Chvostova, V. Proks, F. Rypacek, *Biomacromolecules*, 2011, **12**, 3232.
13) J. P. Blinco, V. Trouillet, M. Bruns, P. Gerstel, H. Gliemann and C. Barner-Kowollik, *Adv. Mater.*, 2011, **23**, 4435.
14) A. P. Hitchcock, J. A. Horsley and J. Stohr, *J. Chem. Phys.*, 1986, **85**, 4835; M. Oçafrain, T. K. Tran, P. Blanchard, S. Lenfant, S. Godey, D. Vuillaume and J. Roncali, *Adv. Funct. Mater.*, 2008, **18**, 2163.
15) A. Vesel, M. Mozetic and A. Zalar, *Vacuum*, 2007, **82**, 248.